trajectory described by the differential equation given by Eq. (1). Note that, in the derivation of Eqs. (14) and (15), no restriction is placed on the time variation of the velocities v_t and v_m of target and missile.

III. Trajectory Equation

Instead of differentiating with respect to time as in Eqs. (6) and (7), one can differentiate with respect to θ by using the following relations:

$$\dot{r} = \dot{\theta}\,\frac{\mathrm{d}r}{\mathrm{d}\theta} \tag{16}$$

$$\ddot{r} = \ddot{\theta}\,\frac{\mathrm{d}r}{\mathrm{d}\theta} + \dot{\theta}^2\,\frac{\mathrm{d}^2 r}{\mathrm{d}\theta^2} \tag{17}$$

By substituting Eqs. (16) and (17) in Eq. (6) for the radial acceleration, one gets the second-order differential equation

$$\frac{\mathrm{d}^2 r}{\mathrm{d}\theta^2} - \frac{2}{r}\left(\frac{\mathrm{d}r}{\mathrm{d}\theta}\right)^2 - \left(1 - \frac{g}{\dot{\theta}^2}\right) r = 0 \tag{18}$$

By substituting Eqs. (14) and (15) into Eq. (18), one gets

$$\frac{\mathrm{d}^2 r}{\mathrm{d}\theta^2} - \left(1 - \frac{\dot{\psi}}{\dot{\theta}}\right)\left(\frac{1}{r}\right)\left(\frac{\mathrm{d}r}{\mathrm{d}\theta}\right)^2 + \frac{\dot{\psi}}{\dot{\theta}} r = 0 \tag{19}$$

When the proportional navigation law $k = \dot{\psi}/\dot{\theta}$, where k is a constant, is used, Eq. (19) integrates to

$$r^k = C|\sin(k\theta + b)| \tag{20}$$

which is similar to the result derived by Lu[6] for the case of a nonmoving target.

On the other hand, if we assume that the radial acceleration in Eq. (6) is zero, then Eq. (18) reduces to

$$\frac{\mathrm{d}^2 r}{\mathrm{d}\theta^2} + \frac{\ddot{\theta}}{\dot{\theta}^2}\frac{\mathrm{d}r}{\mathrm{d}\theta} - r = 0 \tag{21}$$

In the case where the target velocity v_t is constant and horizontal, it is easily shown that $\ddot{\theta}/\dot{\theta}^2 = 2\cot\theta$, which is the case treated by Jalali-Naini and Esfahanian.[7] The solution in this case is given by $r\sin\theta = A_1(\theta - \theta_0)$, and one can easily derive for the transverse acceleration [Eq. (7)] $a_\theta = \dot{l}/r = (2A_1 v_t^2/h)\sin^3\theta$, which is Eq. (22) of Ref. 7 (h is the constant vertical distance of the target from the x axis).

IV. Conclusions

This study shows that some scattered published results in the field of guidance theory can be derived directly from a general differential equation derived from classical mechanics. This approach offers the possibility of allowing a unified approach for various methods used to model the trajectory of a homing missile.

References

[1] Shoucri, R. M., "Elliptical Orbit with Variable Angular Momentum," *Journal of Guidance, Control, and Dynamics*, Vol. 18, No. 5, 1995, pp. 1213–1215.

[2] Shoucri, R. M., "Constant Keplerian Orbit with Non-Central Force Field," *International Journal of Engineering Education*, Vol. 12, No. 4, 1996, pp. 305–308.

[3] Shoucri, R. M., "Note on Kepler's Problem with Variable Angular Momentum," *Celestial Mechanics and Dynamical Astronomy*, Vol. 63, No. 2, 1996, pp. 75–85.

[4] Shoucri, R. M., "Elliptical Orbit with Non-Central Force Field in Celestial Mechanics," *Celestial Mechanics and Dynamical Astronomy*, Vol. 65, No. 4, 1997, pp. 373–388.

[5] Yang, C.-D., Yeh, F.-B., and Chen, J.-H., "The Closed-Form Solution of Generalized Proportional Navigation," *Journal of Guidance, Control, and Dynamics*, Vol. 10, No. 2, 1987, pp. 216–218.

[6] Lu, P., "Intercept of Nonmoving Targets at Arbitrary Time-Varying Velocity," *Journal of Guidance, Control, and Dynamics*, Vol. 21, No. 1, 1998, pp. 176–178.

[7] Jalali-Naini, S. H., and Esfahanian, V., "Closed-Form Solution of Line-of-Sight Trajectory for Nonmaneuvering Targets," *Journal of Guidance, Control, and Dynamics*, Vol. 23, No. 2, 2000, pp. 365, 366.

Output-Rate Weighted Optimal Control of Aeroelastic Systems

Ashish Tewari*

Indian Institute of Technology, Kanpur 208 016, India

Introduction

THE optimal linear quadratic regulator (LQR) problem[1] is the backbone of many modern optimal, robust control design methods, such as the linear quadratic Gaussian procedure with loop-transfer recovery (LQG/LTR)[2] and the H_2/H_∞ control. The output-weighted LQR problem (referred to as LQRY) minimizes an objective function containing the quadratic form of the measured output as an integrand. However, in several applications it may be more desirable to minimize the time rate of change of the output, rather than the output itself. Examples of such active control applications are vibration reduction of flexible structures, flutter suppression, gust and maneuver load alleviation of aircraft, and ride-quality augmentation of any vehicle. In these cases, the measured output is usually the normal acceleration, although it is necessary from consideration of passenger/crew comfort (as well as issues such as weapons aiming and delivery) to have an optimal controller that minimizes the roughness of the motion, which can be defined as the time rate of change of normal acceleration. This mechanical analogy can be extended to other physical systems, where sensor limitations prevent the measurement of time rate of change of an available signal, and even to economic models. Also, it is well known that certain jerky nonlinear motions, if uncorrected, can lead to chaos.[3] Optimal control of such motions may require output-rate weighted (ORW) objective functions.

ORW Optimal Control

Consider a linear time-invariant system described by the following state-space equation:

$$\frac{\mathrm{d}\boldsymbol{X}}{\mathrm{d}t} = \boldsymbol{AX} + \boldsymbol{Bu} + \boldsymbol{Fv} \tag{1}$$

where $\boldsymbol{X}$ is the state vector, $\boldsymbol{u}$ is the input vector, and $\boldsymbol{v}$ is the process noise vector. Then the output vector $\boldsymbol{y}$ is given by

$$\boldsymbol{y} = \boldsymbol{CX} + \boldsymbol{Du} + \boldsymbol{w} \tag{2}$$

where $\boldsymbol{w}$ is the measurement noise vector. The regulator design problem is finding an optimal feedback gain matrix $\boldsymbol{K}$, which obeys the control law

$$\boldsymbol{u} = -\boldsymbol{KZ} \tag{3}$$

where $\boldsymbol{Z}$ is the estimated state vector, such that the following objective function is minimized:

$$J = \left(\frac{1}{2}\right)\int_0^\infty \left[\left(\frac{\mathrm{d}\boldsymbol{y}}{\mathrm{d}t}\right)^T \boldsymbol{Q}\left(\frac{\mathrm{d}\boldsymbol{y}}{\mathrm{d}t}\right) + \boldsymbol{u}^T\boldsymbol{Ru}\right]\mathrm{d}t \tag{4}$$

Equation (4) can be rewritten as

$$J = \left(\frac{1}{2}\right)\int_0^\infty (\boldsymbol{X}'\bar{\boldsymbol{Q}}\boldsymbol{X} + \boldsymbol{X}'\boldsymbol{S}'\boldsymbol{U} + \boldsymbol{U}'\boldsymbol{SX} + \boldsymbol{U}'\bar{\boldsymbol{R}}\boldsymbol{U})\,\mathrm{d}t \tag{5}$$

Received 5 February 1999; revision received 20 April 2000; accepted for publication 2 November 2000.

*Assistant Professor, Department of Aerospace Engineering. Senior Member AIAA.

where

$$\bar{Q} = \bar{C}'Q\bar{C}, \qquad S = \bar{D}'Q\bar{C}, \qquad \bar{R} = R + \bar{D}'Q\bar{D}$$

$$\bar{C} = CA, \qquad \bar{D} = [CB \quad D], \qquad U = \left[u \frac{\mathrm{d}u}{\mathrm{d}t}\right]' \tag{6}$$

Note that the output-weighted LQRY control is a subcase of the general ORW control described by Eqs. (3–6). For strictly proper plants, $\boldsymbol{D} = \boldsymbol{0}$, the performance integral in Eq. (5) reduces to a form similar to that of the general LQRY problem.[1,4]

When the separation principle[2] is followed, the regulator and state estimator are separately designed and then combined to form a compensator. The optimal regulator gain matrix $\boldsymbol{K}$, which minimizes the objective function of Eq. (4) subject to Eq. (1), is given by

$$K = \bar{R}^{-1}(B'M + S) \tag{7}$$

where $\boldsymbol{M}$ is the solution of the following algebraic Riccati equation:

$$M\bar{A} + \bar{A}'M - MB\bar{R}^{-1}B'M + \tilde{Q} = 0 \tag{8}$$

in which

$$\bar{A} = A - B\bar{R}^{-1}S, \qquad \tilde{Q} = \bar{Q} - S'\bar{R}^{-1}S \tag{9}$$

After a regulator is designed by the given procedure, the state-estimator gain matrix $\boldsymbol{K}_e$ is derived for LTR at the plant input[2] such that

$$\frac{\mathrm{d}Z}{\mathrm{d}t} = AZ + Fv + Bu + K_e(y - CZ - Du) \tag{10}$$

where

$$K_e = (NA' + FVF')C'(CFVF'C')^{-1} \tag{11}$$

where $\boldsymbol{V}$ and $\boldsymbol{W}$ are spectral densities of the process and measurement noise, respectively, and $\boldsymbol{N}$ is the solution of the following observer algebraic Riccati equation:

$$AN + NA' - NC'W^{-1}CN + FVF' = \boldsymbol{0} \tag{12}$$

Example: Stability Augmentation of Unstable Elastic Aircraft

The pitching motion of a B-1 bomber with a fuselage bending mode, whose stability and structural data are obtained from Refs. 5 and 6, is modified by making it statically unstable and adding first-order actuators for the two aerodynamic control surfaces, the elevator and the canard. The elevator actuator time lag is assumed to be 1/75 s whereas that for the canard is 1/100 s. The output vector $\boldsymbol{y}$ consists of pitch rate and normal acceleration at the fuselage station 82 ft from the nose. The state-space model is derived at the nominal steady-state flight Mach number 0.6, and standard altitude 5000 ft. For the bomber-type airplane considered here, it is necessary that both pitch rate and normal acceleration should quickly decay to zero when a vertical gust is encountered, because the stability of the bombing platform is crucial for mission success. The ORW controller minimizes pitch acceleration and the time rate of change of normal acceleration. The best case LQRY and ORW controllers are obtained by taking $\boldsymbol{Q} = 10^{-8}\,\boldsymbol{I}_2$ and $\boldsymbol{R} = \boldsymbol{I}_2$. For the ORW controller, the state estimator is derived with $\boldsymbol{F} = \boldsymbol{I}_6$, $\boldsymbol{V} = \boldsymbol{C}'\boldsymbol{C}$, and $\boldsymbol{W} = \boldsymbol{I}_2$. For LQRY observer, $\boldsymbol{F} = \boldsymbol{B}\boldsymbol{B}'$, $\boldsymbol{V} = \boldsymbol{C}'\boldsymbol{C}$, and $\boldsymbol{W} = \boldsymbol{I}_2$. Figure 1 compares the closed-loop fuselage bending displacement ζ at the sensor location. The ORW controller is seen to produce a much smoother bending response, with a smaller overshoot, which decays faster than that of the LQRY controller. Figure 1 is typical for the other transients, for example, pitch rate, pitch acceleration, normal acceleration, time rate of normal acceleration, and canard and elevator deflections.

Example: Active Flutter Suppression

Active flutter suppression of a typical section with a trailing-edge control surface and accelerometer output (Ref. 7), $\mathrm{d}^2\zeta/\mathrm{d}t^2$, is achieved with an ORW compensator designed using $\boldsymbol{Q} = 1$, $\boldsymbol{R} = 1$, $\boldsymbol{F} = \boldsymbol{I}_{12}$, $\boldsymbol{V} = 0.03\boldsymbol{C}'\boldsymbol{C}$, and $\boldsymbol{W} = 1$ and compared with an LQRY compensator designed using $\boldsymbol{Q} = 1$, $\boldsymbol{R} = 1$, $\boldsymbol{F} = \boldsymbol{I}_{12}$, $\boldsymbol{V} = \boldsymbol{C}'\boldsymbol{C}$, and $\boldsymbol{W} = 1$ in Fig. 2, which shows the closed-loop initial response to a

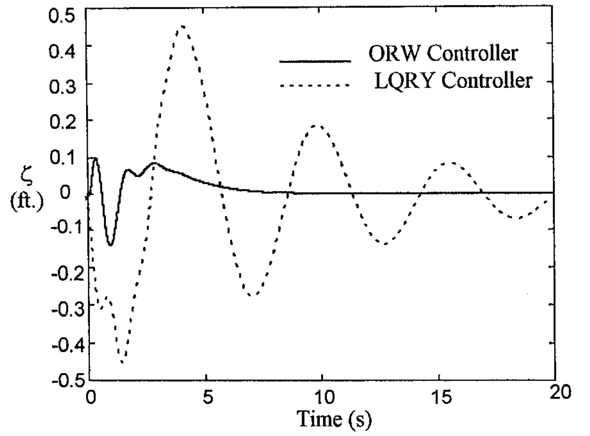

Fig. 1 Closed-loop fuselage bending displacement for the elastic bomber airplane.

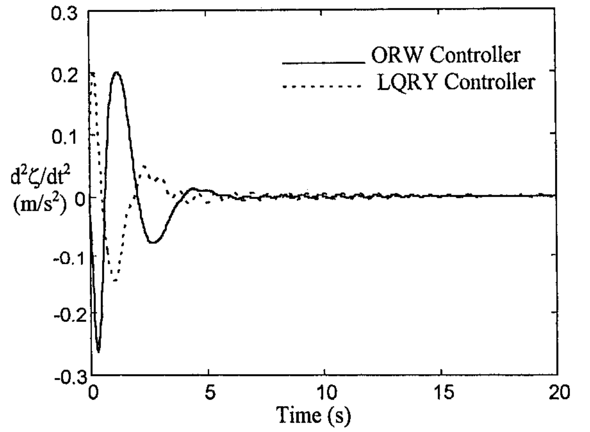

Fig. 2 Closed-loop normal acceleration in active flutter suppression.

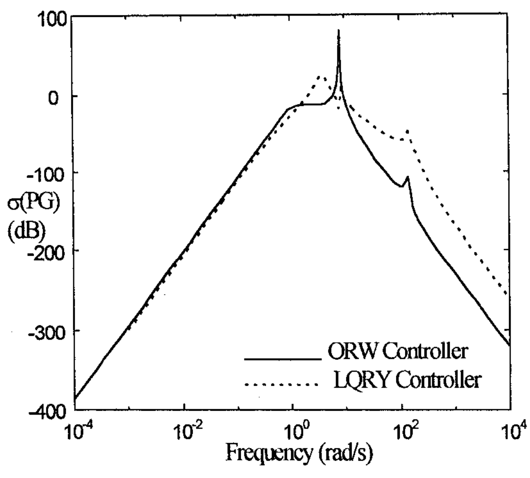

Fig. 3 Singular-value spectrum of controller in series with plant for flutter suppression.

unit nondimensional plunge rate. The ORW response is smoother and decays about 5 s earlier than the LQRY response. Figure 3 compares the singular value of the open-loop sytem, $\sigma[\boldsymbol{P}(s)\boldsymbol{G}(s)]$, for the two controllers, where $\boldsymbol{P}(s)$ and $\boldsymbol{G}(s)$ are the transfer functions of the controller and the plant, respectively, given by

$$P(s) = [K(sI - A + BK + K_eC - K_eDK)^{-1}K_e]$$

$$G(s) = C(sI - A)^{-1}B + D \tag{13}$$

The singular-value peak of the ORW system near the flutter frequency (8.2 rad/s) is much larger than that of the LQRY system, indicating smaller robustness of the ORW controller to process noise close to the flutter point. However, at higher frequencies, the

ORW controller displays a better noise attenuation than the LQRY controller.

Conclusions

The ORW control applied to two aeroelastic systems results in a better performance in terms of smoothness of response and decay time, but a greater sensitivity to process noise when compared to the traditional output-weighted optimal control. Its use may lie in controlling well-modeled plants where robustness is less critical, but where smoothness of response is important for issues such as passenger comfort, or weapons aiming and delivery.

References

[1]Friedland, B., *Control System Design: An Introduction to State-Space Methods*, McGraw–Hill, New York, 1987, pp. 364–365.

[2]Stein, G., and Athans, M., "The LQG/LTR Procedure for Multivariable Feedback Control Design," *IEEE Transactions on Automatic Control*, Vol. 32, 1987, pp. 105–114.

[3]Linz, S. J., "Nonlinear Dynamical Models and Jerky Motion," *American Journal of Physics*, Vol. 65, No. 6, 1997, pp. 523–526.

[4]Zhou, K., and Doyle, J. C., *Essentials of Robust Control*, Prentice–Hall, Upper Saddle River, NJ, 1998, p. 254.

[5]Newman, B., and Schmidt, D. K., "Numerical and Literal Aeroelastic Vehicle Model Reduction for Feedback Control Synthesis," *Journal of Guidance, Control, and Dynamics*, Vol. 14, No. 5, 1991, pp. 943–953.

[6]Waszak, M., and Schmidt, D. K., "Flight Dynamics of Aeroelastic Vehicles," *Journal of Aircraft*, Vol. 25, No. 6, 1988, pp. 563–571.

[7]Tewari, A., "Output Rate Weighted Active Flutter Suppression," AIAA Paper 99-4312, Aug. 1999.

Measurement Rate Reduction in Hybrid Systems

D. D. Sworder*
University of California, San Diego, La Jolla, California 92037
and
J. E. Boyd†
Cubic Defense Systems, San Diego, California 92186

I. Introduction

IN some tracking applications, location estimates are found by first approximating the conditional distribution of the state vector with a Gaussian sum distribution. Gaussian sums have proven their worth in various problems, particularly those with hybrid dynamic models.[1] However, in an encounter involving multiple aircraft, tracked with multiple sensors, and having multiple motion modes, the number of possible hypotheses delineating the temporal evolution of the motion/observation path grows geometrically. If each modal path is associated with an element in a Gaussian sum, the comprehensive conditional density has too many terms. The geometric growth in complexity forces a designer to simplify the distribution through a process of mixture reduction. Several plausible methods of avoiding hypothesis bloating are provided in Ref. 2.

In this Note, the focus is on a single target that is maneuvering in the plane. The maneuver path is created by changing the motion mode of the aircraft, for example, coasting, turning, jinking, and so on. If the modal path were known, conventional methods could be used to estimate the state of the target. However, the unpredictable (and unmeasured) modal dynamics create considerable difficulty.

Received 7 April 2000; revision received 4 September 2000; accepted for publication 16 October 2000.

*Professor, Department of Electrical and Computer Engineering, 9300 Gilman; dsworder@ucsd.edu.

†Chief Scientist, P.O. Box 85587; john.boyd@cubic.com.

To be more specific, suppose the motion model of the target is defined on a particular probability space and the time interval $[0, T]$. There are two right-continuous, random processes: $\{\Phi_t\}$, a piecewise constant modal process ranging over an index set of size $\boldsymbol{S}$, and $\{\boldsymbol{w}_t\}$, a Brownian motion. The modal state ϕ_t is a unit vector in $\mathbb{R}^S$ with state space $\{\boldsymbol{e}_1, \ldots, \boldsymbol{e}_S\}$. The component in ϕ_t with value one marks the current motion mode. The modal dynamics are usually represented by an exogenous Markov model with generator Q'. For notational convenience in what follows, $\boldsymbol{e}_i$ is the ith canonical unit vector in a space whose dimension is obvious from the context. Where no confusion will arise, a subscript may identify time, the component of a vector, or the element of an indexed family with the meaning determined by context; similarly a superscript may denote a power operator or an element of an indexed family. If a process is sampled, the discrete sequence so generated is written $\{\boldsymbol{y}[k]\}$, where the index denotes sample number rather than time. Conditional expectation is denoted with a circumflex, with the relevant σ field apparent from context. A Gaussian random variable with mean $\hat{\boldsymbol{x}}_t$ and covariance P_{xx} is indicated by $\boldsymbol{x} \sim \boldsymbol{N}(\hat{\boldsymbol{x}}_t, \boldsymbol{P}_{xx})$ with the same symbol used for the density function itself where no confusion will arise. If A is a positive symmetric matrix and $\boldsymbol{x}$ a compatible vector, $\boldsymbol{x}'A\boldsymbol{x}$ is denoted $\|\boldsymbol{x}\|_A^2$. Denote the inverse of a (positive) covariance matrix, P, by D; for example, $D_i = (P_i)^{-1}$. If $\boldsymbol{m}$ is a vector of conditional means, the product $D\boldsymbol{m}$ is denoted $\boldsymbol{d}$, for example, $\boldsymbol{d}_i = D_i\boldsymbol{m}_i$.

Both time-continuous and time-discrete models have been used in tracking applications, the latter formed by sampling the relevant variables of the former. The linear, time-discrete hybrid model can be derived from the time-continuous model as in Ref. 1:

$$\boldsymbol{x}[k] = \sum_i (A_i\boldsymbol{x}[k-1] + C_i\boldsymbol{w}[k])\phi_i[k-1] \tag{1}$$

$$\phi[k] = \Pi\phi[k-1] + \boldsymbol{m}[k] \tag{2}$$

where $\{\boldsymbol{w}[k]\}$ is a unit Gaussian white sequence and $\{\boldsymbol{m}[k]\}$ is a martingale increment sequence. The vector $\boldsymbol{x}[k]$ is called the base state to distinguish it from the modal state. The modal transition matrix Π can be computed from Q in the customary way. If the time-continuous models are controllable from the plant noise process in every regime, C_i and A_i are both nonsingular for all i. Label the local plant-noise covariance by $R_\chi(i) > 0$.

In common applications, a sensor gives a linear (or linearizable) measurement of the base-state vector:

$$\boldsymbol{y}[k] = H\boldsymbol{x}[k] + \boldsymbol{n}[k] \tag{3}$$

where $\{\boldsymbol{n}[k]\}$ is a Gaussian white sequence with positive covariance R_x. The measurement rate is determined by the sensor and its utilization policy. The measurements may occur at a different rate than the basic clock rate, usually much slower, and the sensor gain can be made time dependent so that at times of no measurement the observation is uninformative.

The initial plant-state categories are assumed to be independent with probability distributions $\boldsymbol{x}[0] \sim \boldsymbol{N}(\hat{\boldsymbol{x}}[\boldsymbol{0}], \boldsymbol{P}_{xx}[\boldsymbol{0}])$ and $\phi[0] \sim \hat{\phi}[0]$. Denote the filtration generated by the measurements by $\mathcal{G}[k]$. The basic tracking problem is that of estimating $\boldsymbol{x}[k]$ on the basis of $\mathcal{G}[k]$.

Investigators have studied hybrid-state estimation with an emphasis on time-continuous plants and a mix of time-continuous and time-discrete observations. The polymorphic estimator (PME) is a practical algorithm for approximating the $\mathcal{G}_t$-regime probabilities along with those $\mathcal{G}_t$ moments important in path following.[1] The PME is moment based and does not provide the $\mathcal{G}_t$-distribution function of the hybrid state.

The motion model is a hybrid in which the kinematics are represented in the conventional manner, and the mode is represented by a random regime process. Good location estimates are produced at reasonable computational cost by algorithms that approximate the conditional density of the kinematic state using an S-fold Gaussian sum; these are also called path-length-one algorithms because they look back one step in the evolution of the modal process:

$$q[k] = \sum_{l=1}^{S} \alpha_l[k]\boldsymbol{N}(\boldsymbol{m}_l[k], \boldsymbol{P}_l[k]) \tag{4}$$